JISSE
ISSN: 2636-4425

Journal of International Society for Science and Engineering
Vol. 6, No. 3, 59-69 (2024)

JISSE
E-ISSN:2682-3438

Performance Analysis Associated with Experimental Verification of Innovative Poly Lactic Acid Material Developed by Fused Deposition Modeling with Quantitively Filling Strategies

Mohamed Hamoud[1] *, Abou Bakr Elshalakany[2, 3], Ragab A. El-Sehiemy[4], Hussein M.A. Hussein[1,5]

[1] *Mechanical Engineering Department, Faculty of Engineering, Helwan University, Cairo, Egypt*

[2] *Production Engineering and Printing Technology Department, Akhbar El Yom Academy, Giza, Egypt*

[3] *Faculty of Energy and Industrial Technology, October Technological University, Giza, Egypt*

[4] *Electrical Engineering Department, Faculty of Engineering, Kafrelsheikh University, Kafrelsheikh City, Egypt*

[5] *Mechanical Engineering Department, Faculty of Engineering, Ahram Canadian University, 6th of October City, Egypt*

ARTICLE INFO

Article history:
Received: 03-08-2024
Accepted:19-09-2024
Online:12-10-2024

Keywords:
Poly Lactic acid
Fused deposition modeling,
Layered Manufacturing
Filling strategies

ABSTRACT

This paper investigates the influence of various filling strategies and infill percentages on the ultimate tensile strength (UTS) and build time of polylactic acid (PLA) objects produced using Fused Deposition Modeling (FDM). The research focused on three infill percentages: 25%, 50%, and 75%, along with four distinct filling strategies: Cross, Cross 3D, Triangles, and Tri-Hexagon. Tensile test specimens were prepared following ASTM D638 standards, with Ultimaker Cura software employed to determine build times. The findings revealed that the Triangles filling strategy provided the highest UTS at 50% and 75% infill, while the Cross-3D strategy consistently delivered the lowest UTS across all percentages. Regarding build time, the Triangles and Tri-Hexagon strategies were the most efficient, offering the shortest building durations. The study concludes that UTS improves as the infill percentage increases, and it ranks the strategies based on both strength and build time, offering practical insights for optimizing FDM printing parameters for PLA materials, and balancing mechanical performance with manufacturing efficiency.

1. Introduction

Additive manufacturing (AM), also known as 3D printing, is an advanced processing technique to manufacture parts with intricate geometry layer-by-layer using solid 3D CAD modeling, [1,2,3]. Numerous LM technologies were presented in the literature. Digital Light Synthesis (DLS), Stereolithography (SLA), Fused Deposition Modeling (FDM), Selective Laser Sintering (SLS), Selective Laser Melting (SLM), and Electron Beam Melting (EBM), etc. The LM techniques are based on the principles of extrusion followed by three-dimensional (3D) dispensing, controlled 3D fiber dispensing, 3D bioprinting, 3D, plotting, 2D and 3D sheet lamination, material-binder jetting the fusion of powder bed, and photo-assisted, or laser-assisted polymerization. The LM materials include polymers (thermosets, elastomers, thermoplastics), metals and alloys, ceramics, and hydrogels [4]. All technologies shared a standard outline of the building process, depicted in Figure 1, which starts with designing a 3D CAD model, converting it to STL format, slicing it into 2D layers, building the layers one on top of another, and finally post-processing the model to remove the supports and finish the profile [5]. In [6], bumpers of automobiles were prepared from flexible and rigid polyurethanes using DLS and compared with those made by conventional lay-up methods to reveal that both flexible and rigid polyurethane bumpers made by LM outperformed the conventional ones made from glass fiber reinforced (GFR) epoxy resins, concerning the mechanical properties.

* Mohamed Hamoud, Mechanical Engineering Department, Faculty of Engineering, Helwan University, Cairo, Egypt, +201111952362, Dr_hamoud2015@h-eng.helwan.edu.eg

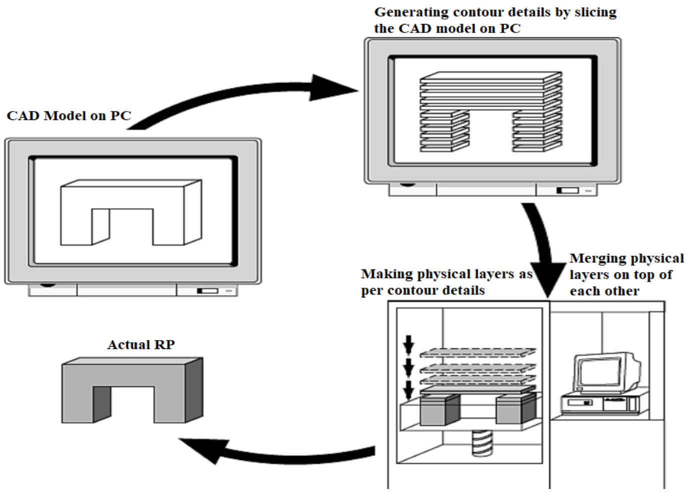

Figure 1: Layered manufacturing process

In FDM, a thermoplastic material is extruded through a nozzle onto a horizontal build platform. The extrusion head piles up very thin blobs of material over the build platform to form the first layer. The platform is maintained at a lower temperature so that the thermoplastic material quickly hardens and fuses with the previous layers, yielding continuity in the material. After the platform lowers, the extrusion head deposits a second layer upon the first; each layer is built on top of the previous one, commencing at the part's base until the desired thickness and shape is obtained. 3DP nylon six blades were prepared for autonomous underwater vehicles by FDM. The prototype exceeded all the design criteria and mechanical properties desirable for such applications, besides giving a corrosion-free, maintenance-free, lightweight, and cost-effective replacement for conventional metallic alloys [7]. FDM technology has some advantages, such as being seen as a desktop printer in a design office since it uses cheap, non-toxic, non-smelling, and environmentally safe materials. There are numerous materials used in FDM, such as PLA (Poly Lactic acid), ABS (acrylonitrile butadiene styrene), PET (polyethylene terephthalate), nylon, PC (polycarbonate), PEI (polyetherimide), and many more [8]. The LM techniques have emerged as a reliable and fast process for polymers, and metallic alloys as print materials are increasingly popular. A recent study on the wear performance of maraging steel developed by Direct Metal Laser Sintering (DMLS) revealed better mechanical properties and wear parameters than the conventional 18Ni1900 steel [9]. The development of a novel material-process combination is much needed in LM to exploit a large combination of process-material and explore new materials, particularly the high-temperature ones like ceramics [10]. While 3DP offers rapid prototyping and pollution-free, low waste fast productivity [11]. The 3DP products often exhibit significant contour errors due to a lack of established process parameters [12]. The applications of 3DP in biomedical areas have also grown increasingly over the last decade due to acceptable cytotoxicity, high dimensional conformance, and printing of customized prosthetics [13]. FDM and pressure-assisted micro syringe (PAM) have been introduced in pharmaceutical industries [14]. Recently, experimental, and theoretical research on the impact of the LM filling methods on mechanical properties is being conducted worldwide. This article concentrates on the study of the material strength of the model built using FDM. There are several studies published in this area. The literature and research database on the process parameters of 3DP process-material is limited to a few only. Rismalia et al. [15] investigated the relationship between fill strategy and filled percentage on the 3DP part developed from PLA. Three fill percentages, 25%, 50%, and 75%, and three filling strategies, grid, tri-hexagon, and concentric, were chosen. Some mechanical properties were studied, such as modules of elasticity, yield point, and UTS. The study concluded that the concentric strategy has the highest values of tensile properties regardless of the filling percentage. Terekhina et al. [16] observed an increasing trend in the mismatch between the theoretical and actual properties with the increase in infill volume. The relationship between the structure of the sample and the limit of its strength was established, together with the effect of internal filling on the strength characteristics of the specimen. Khan et al. [17] studied four different filling strategies to evaluate the mechanical strength of manufacturing specimens. Tensile and three-point bending tests were performed on the printed specimens to examine the tensile and flexural strength. Different filling strategies influenced the mechanical strength of the printed specimen. The study concluded that the rectilinear strategy rendered the highest tensile and flexural strength. V. Mazzanti et al [18] stated that PLA and ABS are the superior materials used with FDM due to their established commercial production, low processing temperature, and near defect-free deposition, but their response to the bio-fillers was not very promising. G. Postiglione et al [19] explained that Besides polymers, polymer-based micro, and nanocomposites have been effectively developed by 3DP, including organic and inorganic Nano fillers. Vishnu et al. [20] studied the honeycomb filling strategy of PLA specimens and evaluated them under various loading conditions to evaluate the mechanical properties and compared the test results of compression strength and impact strength with the printed specimens. The mechanical properties with varying filling percentages were examined, and the microstructural changes predominated the load-bearing conditions. Ramisha Sajjad et al [21] Presented a strategy based on the joining of different infill patterns in a single build part is used to validate the impact of this approach on the strength-to-weight ratio and cost of the manufactured part. Honeycomb, rectilinear, triangle, and rectangular patterns were chosen as individual infill and all possible combinations of these patterns have been examined. Jatinder Singh et al. [22] evaluate the effect of filling percentage and raster style on tensile property of PLA specimen builds at horizontal, on-edge and vertical orientation using open-source 3D printer. L. Feroz Ali et al. [23] In this research work on FDM based additive manufacturing, the main comparison between polyamide 6 (PA6) and polyamide 66 (PA66) is being done to examine the mechanical qualities that lead to low cost, quick, and easy manufacture of components regarding exact aspect. Using the FDM method, test specimens with 50%, 75%, and 100% of infill were made for uncurving constructions, among other percentages. Mohamed Daly et al. [24] This study examines the impact of printing speed on the tensile strength of ABS samples made by the FDM technique. Four different printing speeds—10, 30, 50, and 70 mm/s—were used to assess the mechanical performance of FDM-ABS products. A numerical model was created by using the computer algorithms Abaqus and Digimat to replicate the experimental campaign. This paper also tries to investigate how printing factors affect ASTM D638 ABS specimens. Heba Hussam et al. [25] The goal of this work is to enhance the mechanical characteristics of components manufactured using the fused deposition modeling method. Specimens made of ABS are printed using specific printing parameters. These parameters yield one of the best results yet recorded for 100% infill printed ABS tensile specimens, with a tensile strength that is 86% of the injection-molded ABS strength. Additionally, a post-filling procedure has been investigated. Andrey Yankin et al. [26] In order to increase fatigue resistance, the goal of this research project is to continue optimizing FDM printing parameters for ABS and polyamide (Nylon). Two primary methods are used in the paper's methodology to achieve this goal: finite element analysis and experimental research. The effects of printing internal geometry, printing speed, and nozzle diameter on the fatigue life of ABS and Nylon plastic materials were determined in the experimental section of the article using the Taguchi method.

Previous studies presented good contributions, but the effect of filling strategies and percentages still needs more investigation; new filling strategies have been evaluated. There are only a handful of such articles on the subject. In this study, PLA has been selected as the print material and FDM as LM techniques to explore the effect of filling density and strategies on the printed part's mechanical properties. The objective is to arrive at the highest strength in both high and low filling percentages to help the LM users choose the suitable filling strategy and save the building time and cost, achieving high strength of the part simultaneously. The possibilities to develop complex contours in four different filling strategies have been explored. Further, the study examines the feasibility of reducing the building time and increasing the UTS by changing the filling strategy; and lastly, efforts were made to obtain lower filling percentages for dimensional prototypes to save material, cost, and time.

The main contribution of this study can be summarized as:

1. Introducing different filling strategies for the FDM printer.
2. Experimental verification of the Quantitively filling strategies on four additive filling methodologies, Cross 3D, Triangular, and Tri-Hexagon.
3. An assessment study for the impact of the filling percentages based on different filling methodologies.
4. Develop a new quadratic representation of the UTS in terms of the filling percentages applied for the tested filling methodologies.
5. Investigate a wide range of filling percentages based on the developed mathematical representation and identify the allowable minimum and maximum UTS bounds.
6. Ease of Use

2. Building 3D Printed Specimens Methodology

The 3DP polymer specimens were developed using PLA material, and FDM process, three infill percentages, 25, 50, and 75, and four types of filling methodologies, Cross, Cross 3D, Triangular, and Tri-Hexagon were chosen as shown in Figure 2 (a) to (d). The specimens were printed using a Cartesian FDM printer shown in Figure 3 as per the equipment specifications, Table 1.

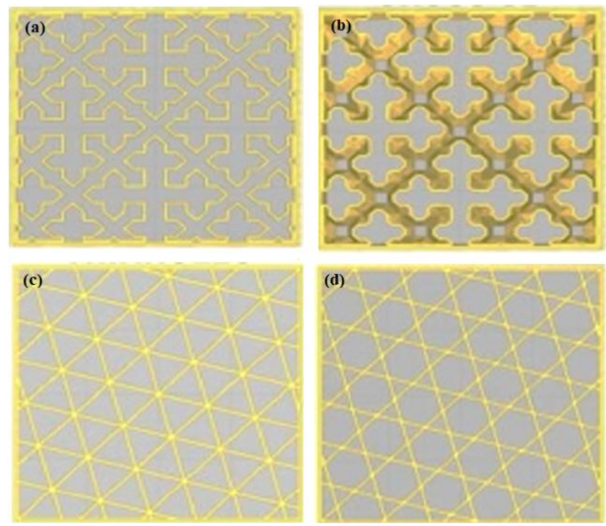

Figure 2: The four types of filling strategies. (a) Cross (b) Cross 3D (c) Triangular and (d) Tri-hexagonal

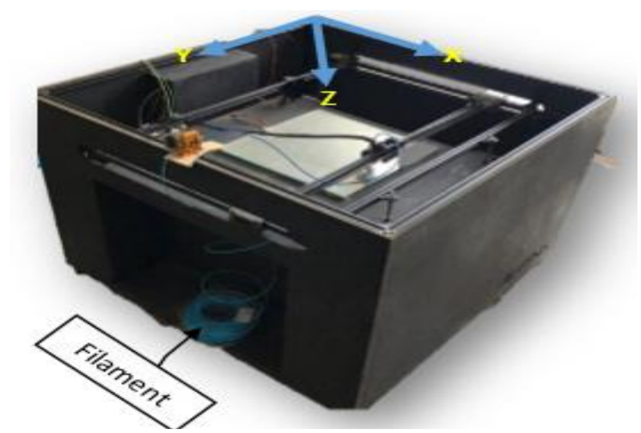

Figure 3: Cartesian FDM Printer

The constant parameters such as PLA filament diameter 1.75 mm, with nozzle temperature 205 °C were used. The filament diameter was decided based on the nozzle size, and the extrusion temperature was fixed per the filament specifications (melting point).

Table 1: Specifications of 3DP FDM machine

Technology	FDM
Build volume	500 mm x 500 mm x 600 mm
Layer thickness	0.2 – 0.4 mm
No. of extruders	1
Diameter of filament	1.75 mm
Types of material	ABS - PLA
Support material	No support
Nozzle diameter	0.4 mm
Power requirements	24 - 30 V

3. Experimental Testing

The tensile test specimens' design was as per the ASTM D638-Type I standard, given in Figure 4. The parameters used in the building specimens were determined using Cura version 5.1.0 software, given in Table 2, and the pictures of the actual specimens after the printing process are shown in Figure 5.

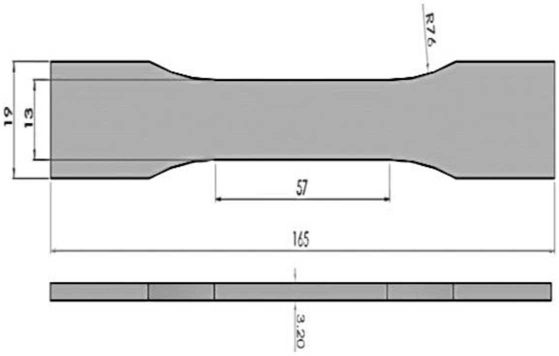

Figure 4: The dimensions of tensile test specimen as per ASTM D638-Type I standard

Figure 5: The printed specimens with Cross 3D infill type with different percentages

Table 2: FDM parameters for printing tensile specimens

Parameter	Value
Layer Thickness	0.2 mm
No. of top and bottom layers	3
Thickness of Wall	1.2 mm
The of Top and Bottom	0.6 mm
Temperature of Printing	205^oC
The temperature of Building Plate	60^oC
Print Speed	20 mm/s

The ASTM D638 type I standard test method was employed for tensile testing of the specimen using W+b Walter + bai ag (LFM-L 20KN) testing machine, shown in Figure 6. The results of tests were documented as the load against elongation, which was later converted into stress-strain curves. The stress points were calculated by converting the elongation into strain by dividing it by the initial length; subsequently, UTS values were obtained from the stress-strain plot.

Figure 6: Testing machine

4. Results and Experimental Validation

The strength (stress) versus the position (elongation) plots are given as separate pictures in Figures 7 to 10 for twelve samples, developed by a combination of three filling percentages, 25%, 50%, and 75%, and four filling strategies, Cross 3D, Triangular, and Tri-hexagon. Many curves were overlapping, so each one was separately given. All materials exhibit ductile behavior, extending a long way before yielding.

a) *Results for Cross-filling strategy*

among Cross filling strategy, shown in Figure 7 (a) to (c), 75% filling gave slightly higher strength before fracture with lesser extension while the 25% filling gave maximum extension before fracture exhibiting most minor strength. The yield point is quite near to the UTS with 75% filling.

b) *Results for Cross 3D filling strategy*

In the Cross-3D filling strategy, shown in Figures 8 (a) to (c), UTS increases with different filling percentages, but there is minimal difference in the extension; overall, the comparison indicates that the Cross-3D at 75% filling percentage is superior to others.

c) Results for Triangular strategy

Figures 9 (a) to (c), give the stress-position curves of Triangular filling strategies at a different filling percentage. As the filling percentage increases, the UTS increases while there is negligible variation in elongation; 75% filling with the Triangular strategy exhibits maximum UTS.

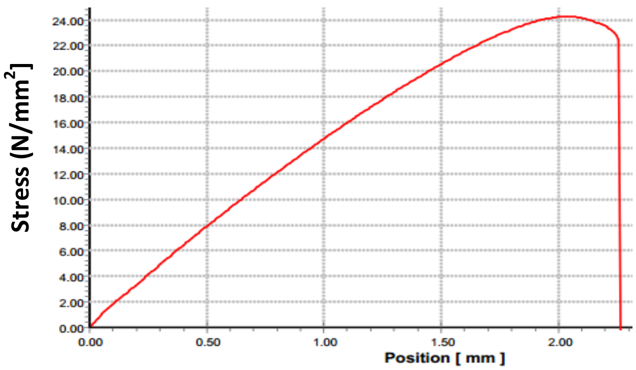

(a) Cross 25 %

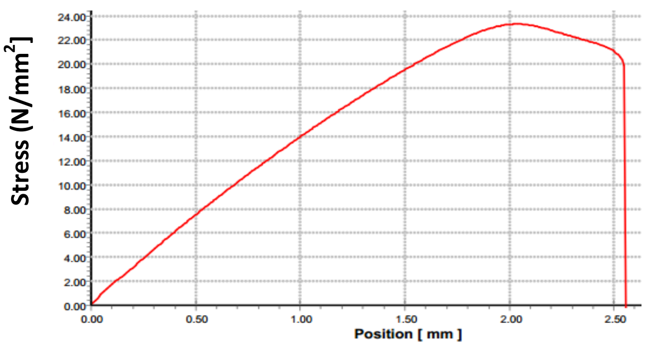

(b) Cross 50 %

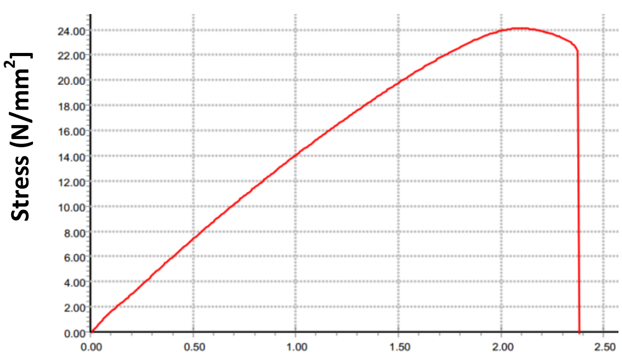

(c) Cross 75 %

Figure 7: Stress-position curves for Cross filling strategy and fill percentages of the specimens

d) Results for the Tri-hexagon filling strategy

In the Tri-hexagon filling strategies, given in Figure 10 (a) to (c), the maximum UTS is exhibited by 75% filling, but the extension is minimal at this filling percentage. In all four filling strategies, the yield stress is close to the UTS at 75 % filling while there is minimal difference in extension, or the extension reduces at UTS.

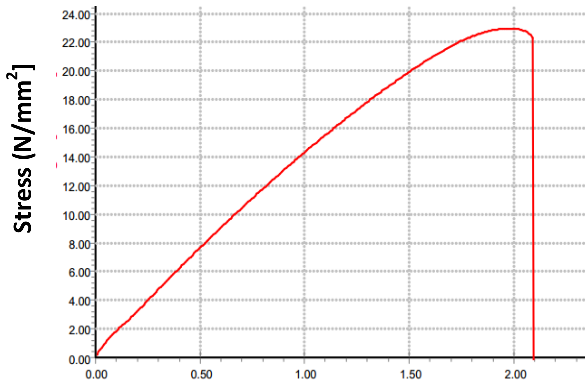

(a) Cross 3D 25 %

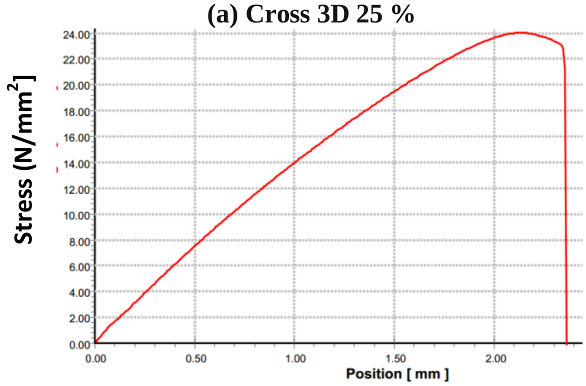

(b) Cross 3D 50 %

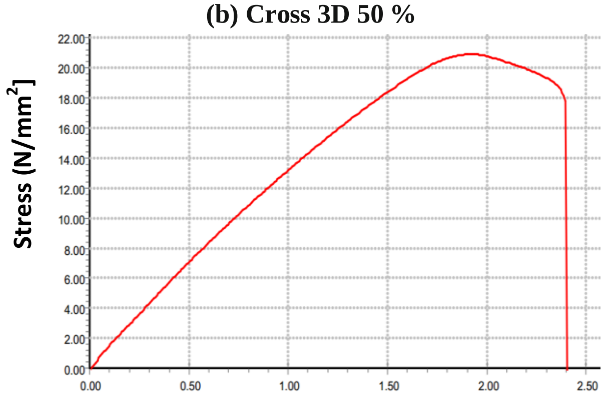

(c) Cross 3D 75 %

Figure 8: Stress-position curves for Cross 3D filling strategy for three fill percentages of the specimens

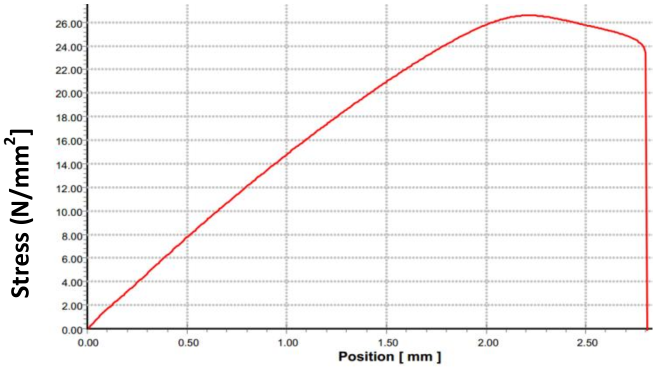

(a) Triangles 25 %

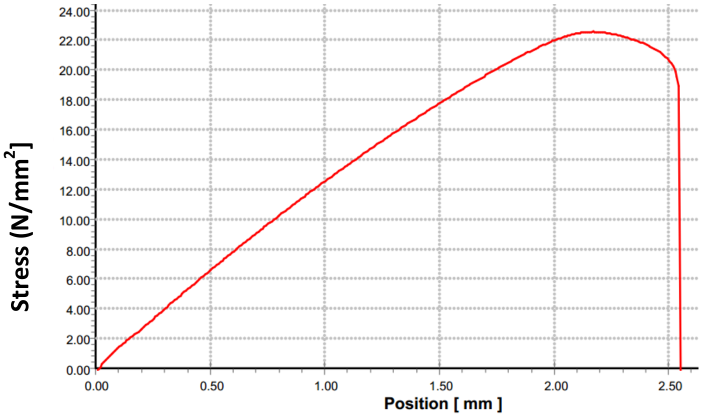

(a)Tri-Hexagon 25%

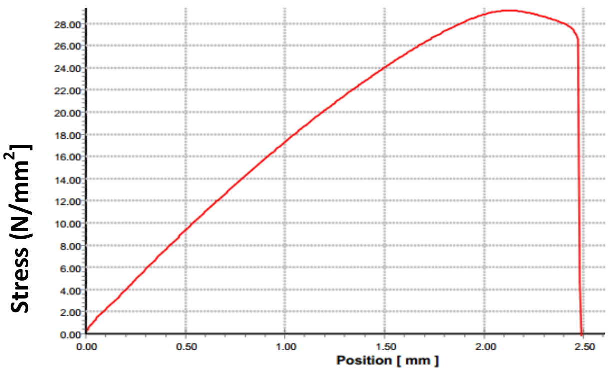

(b) Triangles 50 %

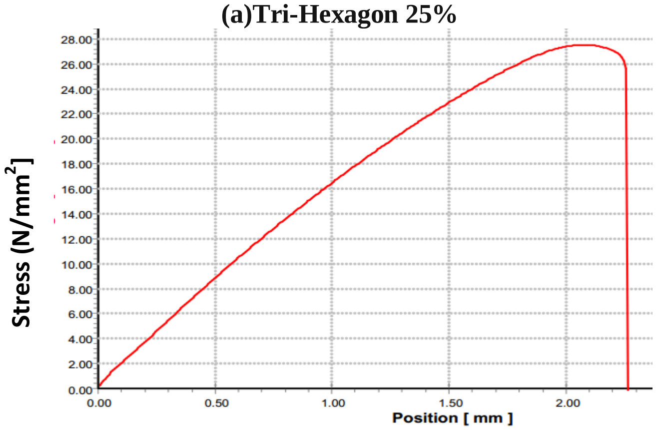

(b)Tri-Hexagon 50%

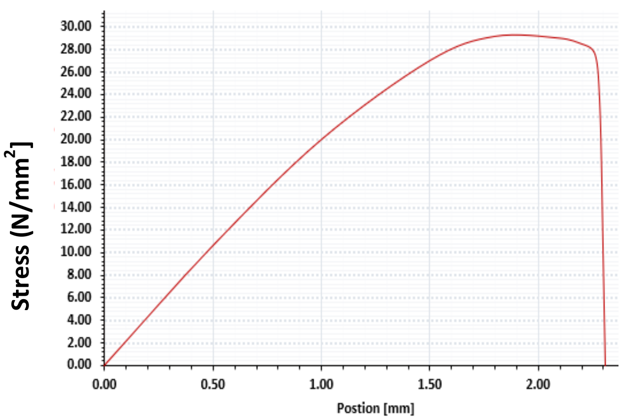

(c) Triangles 75 %

Figure 9: Stress-position curves for Triangles filling strategy and for three fill percentages of the specimens

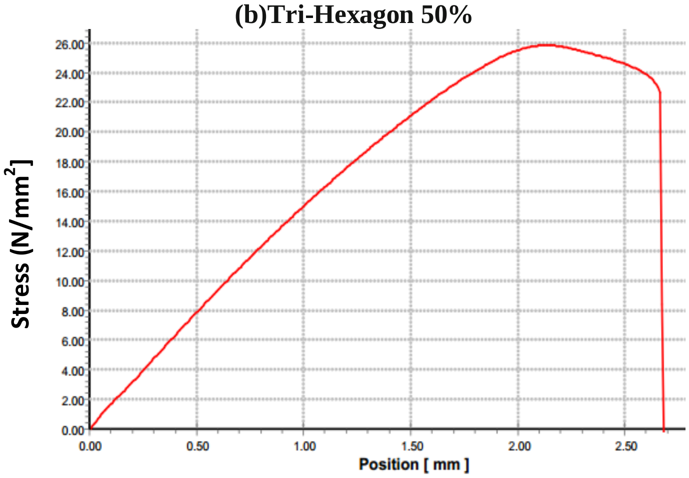

(c)Tri-Hexagon 75%

Figure 10: Stress-position curves for Tri-Hexagon filling strategy for three fill percentages of the specimens

5. Assessment of Filling Strategies

Figure 11 presents the stress-strain curves of all four filling strategies at different infill percentages. The 75% infill percentage gives maximum UTS. The comparison of stresses between filling strategies and filling percentages within the same tensile parameters are listed in Table 3. The maximum UTS is 29.16 MPa, exhibited by Triangular filling at 75%, and the minimum is exhibited by Cross 3D filling (20.8 MPa). There is a gradual increase in the UTS with the filling percentage. The maximum strain at fracture (0.048) is exhibited by Triangular and Tri-hexagonal, while Cross and Cross 3D exhibit the maximum strain of 0.044 at fracture. Strength is a significant limiting criterion for the applications of polymers; the selection of optimum infill percent and filling strategy empowers the designers to select polymers as the candidate materials for product design. The UTS values have been identified and given in Table 4. A comparison of the UTS across different filling strategies, and at different infill percentages is given in Table 5. The triangular filling strategy outperforms all other strategies, and the 75% infill amount is the best among the tested specimens for the UTS values. The curves result and tendency shows that the UTS increases while the filling percentage increases.

Table 3: Conversion table from stress–position relationship to UTS

Position [mm]	Strain	Strategy type	Stress (MPa)		
			25%	50%	75%
0	0	Cross	0	0	0
0.5	0.01		7.6	7.6	8
1	0.02		14	14	14.8
1.5	0.03		19.6	20	22.8
2	0.04		23.3	24	24.4
2.2	0.044		22.6	24.11	24
0	0	Cross 3D	0	0	0
0.5	0.01		7.2	7.6	7.6
1	0.02		13.2	14.2	14
1.5	0.03		18.4	20	19.6
2	0.04		20.8	22.8	23.6
2.1	0.044		20	22	24
0	0	Triangle	0	0	0
0.5	0.01		8	8	9.2
1	0.02		14.8	14.8	17.2
1.5	0.03		19.2	22.8	24
2	0.04		20.3	26	29
2.2	0.044		21.4	26.5	29.16
2.4	0.048		20.4	26	28
0	0	Tri-Hexagon	0	0	0
0.5	0.01		6.4	8	9
1	0.02		12.8	15	16.4
1.5	0.03		17.6	21	22.8
2	0.04		22	25.2	27.3
2.2	0.044		22.56	25.84	27.53
2.3	0.048		22	24.8	26.8

The difference in UTS from 25% to 75% varies from 1.07 to 4.97 MPa. In Cross strategy, there is a 0.44 MPa difference from 50% to 75%. On the other hand, the difference is increased to be 1.2 MPa for the Cross 3D, while for Tringles and Tri-hexagon the difference is 2.66 and 1.69 MPa, respectively. The trends depicted in Figure 11 indicate that a higher filling percentage infers higher resistance to applied internal stresses. Based on the results, the highest UTS corresponded to the Triangles filling strategy with a 75% filling percentage, where it has 29.16 MPa UTS, besides, in the case of lightweight construction at 25% percentage, the triangles-fill strategy is better where it has 26.4 MPa, compared with cross, Cross 3D, and Tri-hexagon which have23.33, 20.8, and 22.56 MPa, respectively with 13 min as minimum building time.

Table 4: UTS Values of the Tested Specimens

Filling Strategy	Filling Percentage	UTS (MPa)	Building Time (Min)	Material (gram)	Consumed Filament (m)
Cross	25%	23.33	17	11	3.65
	50%	24.11	21	12	3.87
	75%	24.4	25	12	4.06
Cross 3D	25%	20.8	17	11	3.62
	50%	22.8	19	11	3.83
	75%	24	25	12	4.06
	25%	21.4	15	11	3.6
Triangles	50%	26.5	17	12	3.89
	75%	29.16	20	13	4.2
Tri-hexagonal	25%	22.56	15	11	3.59
	50%	25.84	17	12	3.89
	75%	27.53	20	13	4.2

Table 5: A comparison of UTS for different percentages and different filling strategies

Type / Percentage	Cross		Cross 3D		Triangles		Tri-Hexagon	
	UTS	Time	UTS	Time	UTS	Time	UTS	Time
At 25%	23.33	17	20.8	17	21.4	11	22.56	11
At 50%	24.11	21	22.8	19	26.5	12	25.84	12
At 75%	24.4	25	24	25	29.16	13	27.53	13

6. Predication Trend Models

The mathematical representation of UTS in terms of the filling percentage (F) can be represented in Table 6 for the four-filling patterns called cross, cross 3D, triangular, and the tri-hexagon. Figures 12 to 15 provide the fitting curves for the four filling patterns. The collected curves based on the given fitting equations for each pattern are shown in Figure 16 for a varied fill in ratio between 0- 100 %. The maximum infill of each pattern can be optimized to find the optimal UTS and employed by using MATLAB environment. The minimum UTS bounds for cross, cross 3D, triangular, and Tri-hexagon patterns are 22.06, 33.2, 13.86, and 17.63 while the maximum UTS bounds are 24.414, 18.64, 29.601, and 27.7852, respectively. The Triangular filling strategy exhibited a maximum UTS of 26.8 MPa at (50%), and 29.16 MPa at (75%). while the Cross 3D filling strategy has the lowest value of UTS at all percentages. It gave 20.8 MPa at (25%), 22.8 MPa at (50%), and 24 MPa at (75%).

Table 6: Mathematical representation of UTS for different patterns

Pattern	UTS in MPa	R^2	SSE
Cross	UTS = -0.00039 F^2 + 0.0606 F + 22.06	1	0
Cross 3D	UTS = -0.00064 F^2 + 0.128 F + 18	1	0
Triangle	UTS = -0.00195 F^2 + 0.3504 F + 13.86	1	0
Tri-Hexagon	UTS = -0.0013 F^2 + 0.2298 F + 17.63	1	0

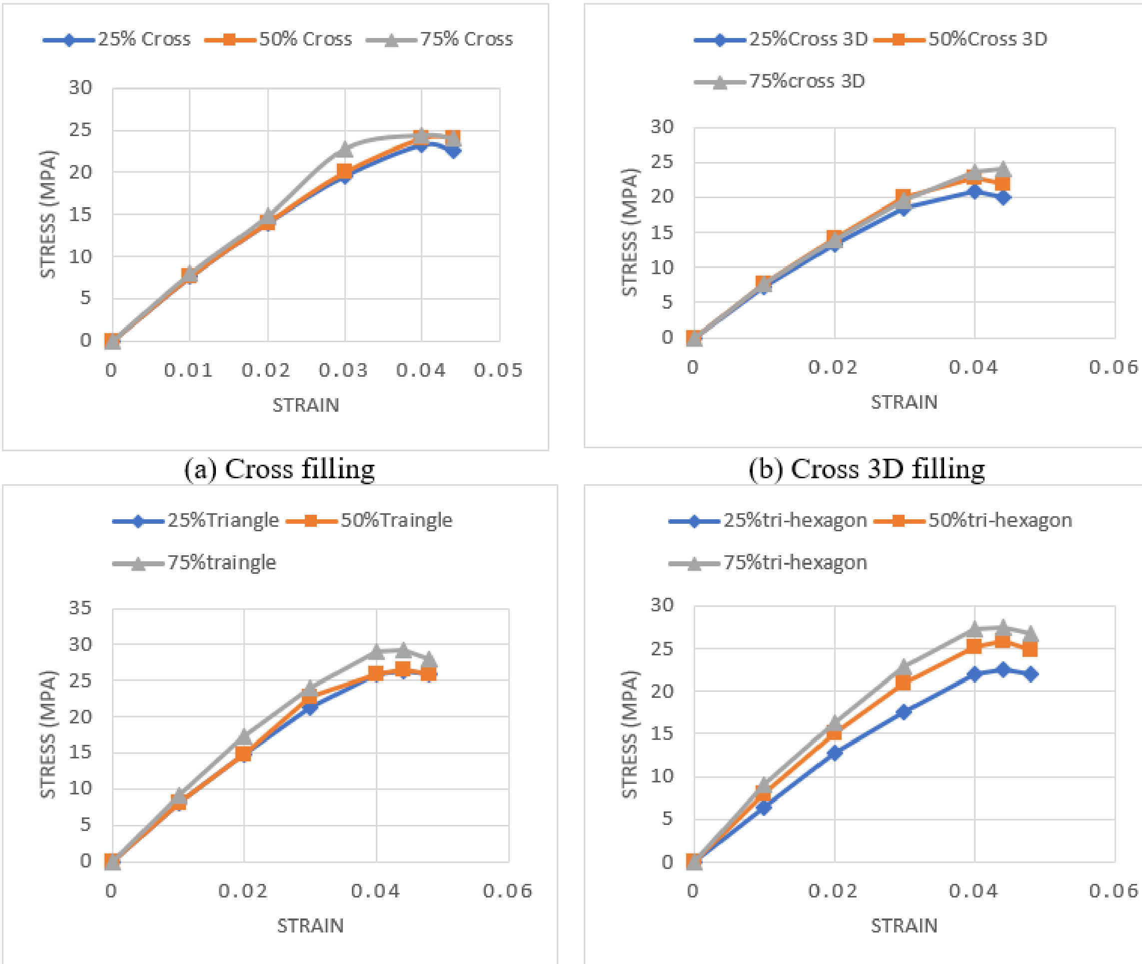

(a) Cross filling

(b) Cross 3D filling

(c) Triangular filling

(d) Tri-hexagon filling

Figure 11: Stress-strain curves for all four filling strategies and infill percentage

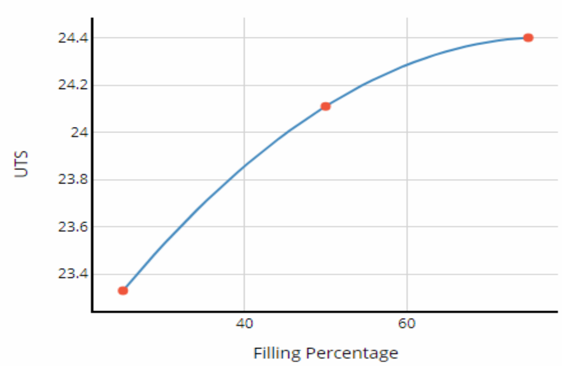

Figure 12: Fit curve for cross filling pattern

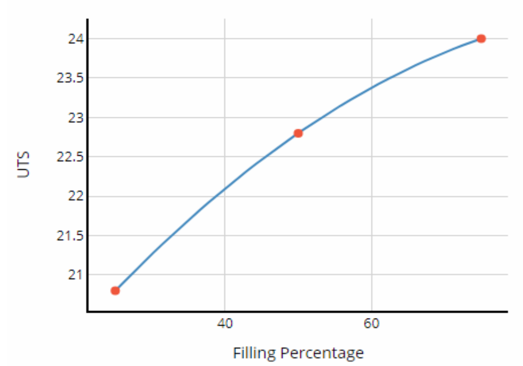

Figure 13: Fit curve for cross 3D filling pattern

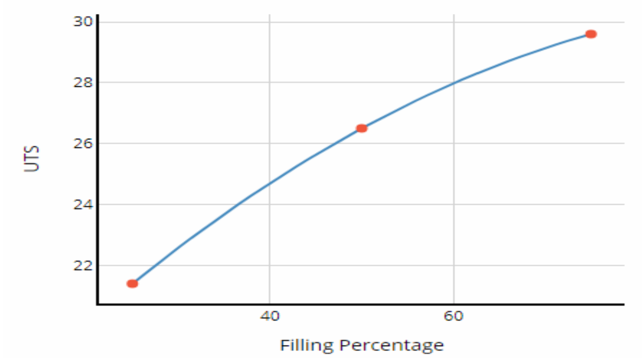

Figure 14: Fit curve for Triangle filling pattern

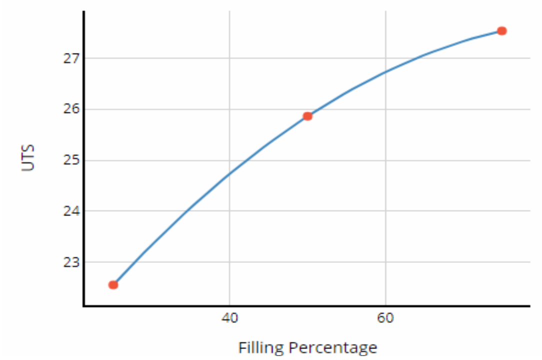

Figure 15: Fit curve for Tri-Hexagon filling pattern

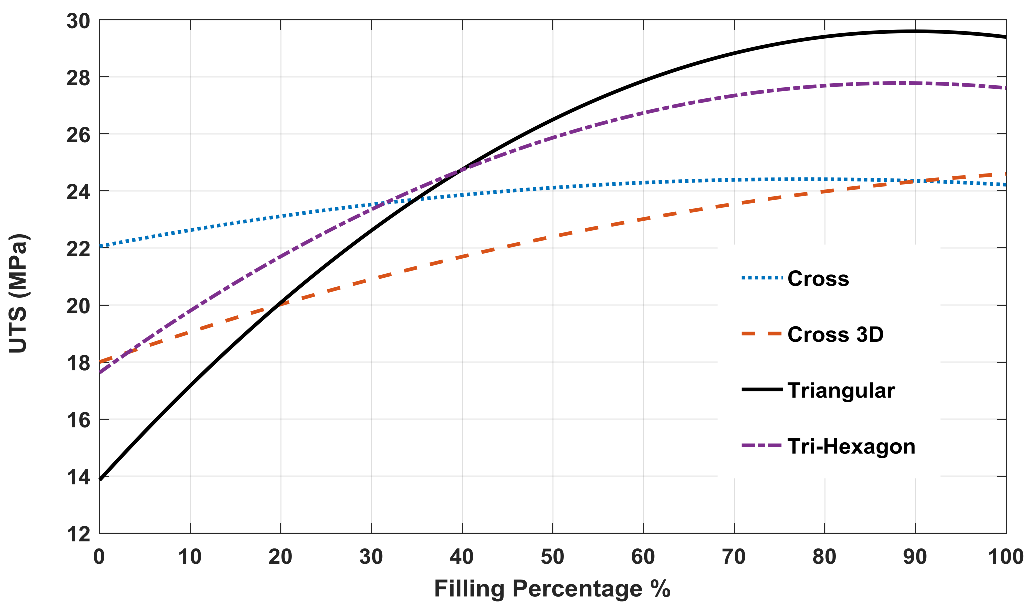

Figure 16: Wide range Fitting curves of different filling patterns

7. Conclusions

Tensile samples were printed using PLA material via the FDM-LM process to evaluate the ultimate tensile strength (UTS) and build time across four filling strategies and three infill percentages. The experimental results showed that both the filling strategy and infill percentage significantly impacted UTS and built time. The Tri-Hexagon and Cross strategies generally yielded intermediate UTS values between Triangles and Cross 3D, with the Tri-Hexagon outperforming Cross at higher infill percentages.

In terms of build time, the Triangles and Tri-Hexagon strategies consistently resulted in the shortest times, requiring 11, 12, and 13 minutes for 25%, 50%, and 75% infill, respectively. It was also observed that UTS increased as the infill percentage increased across all four strategies. The strength ranking of the strategies is as follows: Triangles exhibited the highest UTS, followed by Tri-Hexagon, Cross, and finally, Cross 3D, which had the lowest strength values. Regarding build time, Triangles and Tri-Hexagon had the shortest times, followed by Cross 3D, with Cross having the longest times.

These findings can serve as a reference for Layered Manufacturing (LM) users to optimize building parameters based on the required strength, cost, and build time. Furthermore, the relationship between UTS and infill percentage is nonlinear, with the Triangles strategy showing a more significant UTS improvement as the infill percentage increases compared to the other strategies. The study suggests using higher infill percentages to explore further improvements in UTS and to evaluate other mechanical properties. A recommended infill range for Triangles is between 50% and 75% for achieving high strength and minimal build time in PLA-based 3D-printed products. Future work can expand on this by combining multiple infill patterns within the same specimen and testing other mechanical properties under varying building parameters.

Conflict of Interest

The authors declare no conflict of interest.

References

[1] Ch Kapil Ror, Vishal Mishra, Sushant Negi, and Vinyas M, (2024), "Utilizing in-nozzle impregnation for enhancing the strength of recycled PET-derived 3D printed continuous banana fiber reinforced bio-composites", Rapid Prototyping Journal. https://doi.org/10.1108/RPJ-10-2023-0379

[2] Hamoud and Sobhi, (2022)," A new algorithm for optimal process parameters based on minimum building time in additive manufacturing", Beni-Suef Univ J Basic Appl Sci https://doi.org/10.1186/s43088-022-00260-w

[3] A. V. Ripetskiy, E. V. Mikhailova, D. V. Fedoseev, N. Yu. Temicheva, and S. A. Sitnikov, (2023), "Predictive Modelling of Surface Roughness in Layered Manufacturing Using H15N5D4B and KH28M6", E3S Web of Conferences 413, 04017. doi: https://doi.org/10.1051/e3sconf/202341304017

[4] S. C. Ligon, R. Liska, J. Stampfl, M. Gurr, and R. Mülhaupt, (2017), "Polymers for 3D Printing and Customized Additive Manufacturing", Chem. Rev., 117, 10212. doi: 10.1021/acs.chemrev.7b00074

[5] M. Hamoud, A. EL-Wahab, and A. Barakat, (2016), "Speeding Up Algorithm for Building the STL Model Using 3D Printing", Int. Conf. Appl. Mech. Eng, 17, 1. doi: 10.21608/amme.2016.35356

[6] S. Begum, G. M. S. Ahmed, I. A. Badruddin, V. Tirth, and A. Algahtani, (2019), "Analysis of Digital Light Synthesis Based Flexible and Rigid Polyurethane for Applications in Automobile Bumpers", Mater. Express, 9, 839. doi: 10.1166/mex.2019.1578.

[7] H.M.T. Khaleeda, Irfan Anjum Badruddinb, A.N. Saquiba, Ali E. Anqib, Vineet Tirthb, M.F. Addasa, Faisal O. Mahroogia, Sarfaraz Kamangarb, T.M. Yunus Khanb, Amro Hamada Ma, Amin A.G. Haidera (2020), "Finite Element Analysis of Nylon Based 3D Printed Autonomous Underwater Vehicle Propeller", Mat. Exp., 23. https://doi.org/10.1590/1980-5373-MR-2020-0236

[8] M. Hamoud, (2018), "Surface Roughness Justification in Additive Manufacturing", Int. Conf. Appl. Mech. Mech. Eng., 18, 1. doi: 10.21608/amme.2018.35011.

[9] G. M. S. Ahmed, I. A. Badruddin, V. Tirth, A. Algahtani, and M. A. Ali, (2020), "Wear Resistance of Maraging Steel Developed by Direct Metal Laser Sintering", Mater. Express, 7, 1079. doi: 10.1166/mex.2020.1715.

[10] B. R. Utela, D. Storti, R. L. Anderson, and M. Ganter, (2010), "Development Process for Custom Three-Dimensional Printing (3DP) Material Systems", J. Manuf. Sci. Eng. Trans. ASME 2010, 132, 0110081. doi: 10.1115/1.4000713.

[11] S. Li and S. Cao, (2012), "Print Parameters Influence on Parts' Quality and Calibration with 3DP-Part I: Print Parameters Influence on Parts' Surface Topography", Adv. Mater. Res., 399, 1639. doi: 10.4028/www.scientific.net/AMR.399-401.1639.

[12] S. Li and S. Cao, (2012), "Print Parameters Influence on Parts' Quality and Calibration with 3DP-Part II: Print Parameters Calibration and Contour Accuracy Control", Adv. Mater. Res., 399, 1687. doi: 10.4028/www.scientific.net/AMR.399-401.1687.

[13] J. Singh, P. M. Pandey, T. Kaur, and N. Singh, (2020), "Surface Characterization of Polycaprolactone and Carbonyl Iron Powder Composite Fabricated by Solvent Cast 3D Printing for Tissue Engineering", Polym. Compos., 42, 1. doi: 10.1002/pc.25871.

[14] M. A. Azad, D. Olawuni, G. Kimbell, A. Z. M. Badruddoza, M. S. Hossain, and T. Sultana, (2020), "Polymers for Extrusion-Based 3D Printing of Pharmaceuticals: A Holistic Materials–Process Perspective", Pharma., 12, 124. doi: 10.3390/pharmaceutics12020124.

[15] M. Rismalia, S. C. Hidajat, I. G. R. Permana, B. Hadisujoto, M. Muslimin, and F. Triawan, (2019), "Infill Pattern and Density Effects on the Tensile Properties of 3D Printed PLA Material", J. Phys. Conf. Ser., 1402. doi: 10.1088/1742-6596/1402/4/044041.

[16] S. Terekhina, I. Skornyakov, T. Tarasova, and S. Egorov, (2019), "Effects of the Infill Density on the Mechanical Properties of Nylon Specimens Made by Filament Fused Fabrication", Technologies, 7, 57. doi: 10.3390/technologies7030057.

[17] S. F. Khan, H. Zakaria, Y. L. Chong, M. A. M. Saad, and K. Basaruddin, (2018), "Effect of Infill on Tensile and Flexural Strength of 3D Printed PLA Parts", IOP Conf. Ser. Mater. Sci. Eng., 429. doi: 10.1088/1757-899X/429/1/012101.

[18] V. Mazzanti, L. Malagutti, and F. Mollica, (2019), "FDM 3D Printing of Polymers Containing Natural Fillers: A Review of Their Mechanical Properties", Polymers (Basel)., 7, 1094. doi: 10.3390/polym11071094.

[19] G. Postiglione, G. Natale, G. Griffini, M. Levi, and S. Turri, (2017), "UV-Assisted Three-Dimensional Printing of Polymer Nanocomposites Based on Inorganic Fillers", Polym. Compos., 38, 1662. https://doi.org/10.1002/pc.23735.

[20] B. V. V. Naidu and G. D. Kumar, (2018), "Additive Manufacturing of Honeycomb Structure and Analysis of Infill and Material Characteristics", Int. J. Sci. Res. Rev, 7, 226.

[21] Ramisha Sajjad, Sajid Ullah Butt, Hasan Aftab Saeed, Muhammad Tuoqeer Anwar, Tahir Rasheed, (2023), "Impact of Multiple Infill Strategy on the Structural Strength of Single Build FDM Printed Parts", Journal of Manufacturing Processes, 89, 105-110. https://doi.org/10.1016/j.jmapro.2023.01.065.

[22] Jatinder Singh, Kapil Kumar Goyal, Rakesh Kumar, (2022), "Effect of Filling Percentage and Raster Style on Tensile Behavior of FDM Produced PLA Parts at Different Build Orientation", Materials Today: Proceedings 63, 433–439. https://doi.org/10.1016/j.matpr.2022.03.444

[23] L. Feroz Ali, R. Raghul, M. Yogesh Muthu Ram, V. Harshavardhan Reddy, N. Shakil Kanna, (2022), "Evaluation of the Polyamide's Mechanical Properties for Varying Infill Percentage in FDM Process", Materials Today: Proceedings 68, 2509–2514. https://doi.org/10.1016/j.matpr.2022.09.227

[24] Mohamed Daly, Mostapha Tarfaoui, Manel Chihi, Chokri Bouraoui, (2023), "FDM Technology and the Effect of Printing Parameters on the Tensile Strength of ABS Parts", The International Journal of Advanced Manufacturing Technology (2023) 126:5307–5323. https://doi.org/10.1007/s00170-023-11486-y.

[25] Heba Hussam, Yasser Abdelrhman, M.-Emad S. Soliman, Ibrahim M. Hassa-Allah, (2022), "Effects of a New Filling Technique on the Mechanical Properties of ABS Specimens Manufactured by Fused Deposition Modeling", The International Journal of Advanced Manufacturing Technology, 121:1639–1650. https://doi.org/10.1007/s00170-022-09351-5.

[26] Yankin, A.; Serik, G.; Danenova, S.; Alipov, Y.; Temirgali, A.; Talamona, D.; Perveen, A. (2023), "Optimization of Fatigue Performance of FDM ABS and Nylon Printed Parts", Micromachines, 14, 34. https://doi.org/10.3390/mi1402030